AC fault ride through control strategy on inverter side of hybrid HVDC transmission systems

Zexin ZHOU[1,2], Zhengguang CHEN[1,2] (iD), Xingguo WANG[1,2],
Dingxiang DU[1,2], Guosheng YANG[1,2], Yizhen WANG[3],
Liangliang HAO[4]

MPCE

Abstract Hybrid high-voltage direct current (HVDC)
transmission systems employ a new type of HVDC trans-
mission topology that combines the advantages of the line-
commutated converter system and the voltage-source
converter system. They can improve the efficiency and
reliability of long-distance power transmission. However,
realizing alternating-current (AC) grid-fault ride through
on the inverter side of a hybrid HVDC transmission system
is a challenge considering that a voltage-source converter
based HVDC (VSC-HVDC) is used on the inverter side. In
this study, a control strategy for an overvoltage fixed
trigger angle based on the power-balance method is
developed by fully utilizing the operation characteristics of
a hybrid HVDC transmission system. The strategy reduces
the inverter-side overvoltage of the HVDC system under a
fault in the inverter-side AC system. Simulations based on
Gezhou Dam are conducted to validate the effectiveness of
the proposed strategy.

✉ Zhengguang CHEN
chenzhengguang@epri.sgcc.com.cn

Zexin ZHOU
zhouzx@epri.sgcc.com.cn

Xingguo WANG
wangxingguo@epri.sgcc.com.cn

Dingxiang DU
dudingxiang@epri.sgcc.com.cn

Guosheng YANG
yangguosheng@epri.sgcc.com.cn

Yizhen WANG
yizhen.wang@tju.edu.cn

1 Introduction

Line-commutated converter based high-voltage direct
current (LCC-HVDC), which is based on thyristor tech-
nology, has been widely used in remote and large-capacity
transmission and asynchronous interconnection but has the
problem of commutation failure on the inverter side [1].
Voltage-source converter based high-voltage direct
current (VSC-HVDC) has developed rapidly, and owing to its
independent control of active and reactive power, it can
work in passive systems without the influence of commu-
tation failure. However, it is expensive, and the running loss
is very high [2, 3]. The hybrid high-voltage direct current
(HVDC) transmission system (LCC-VSC) is a new type of
HVDC transmission topology. It combines the advantages
of LCC and VSC and can improve the operation

Liangliang HAO
llhao@bjtu.edu.cn

[1] China Electric Science Research Institute Co., Ltd., Beijing,
China

[2] State Key Laboratory for Power Grid Safety and Energy
Conservation, Beijing, China

[3] School of Electrical Engineering and Automation, Tianjin
University, Tianjin, China

[4] College of Electrical Engineering, Beijing Jiaotong
University, Beijing, China

characteristics of the alternating current (AC) system on the VSC side. Therefore, it is suitable for the construction of the ultra-high voltage direct current (UHVDC) project and the reformation of the LCC-HVDC project and exhibits good potential for engineering applications [4–7].

In a LCC-VSC, an LCC-HVDC is generally used on the rectifier side, and a VSC-HVDC is employed on the inverter side [8, 9]. Given that a VSC has modular capacitance, when the input power of the HVDC side does not match the output power of the AC side, the power imbalance causes a change in the capacitance voltage of the VSC submodule and a change in the HVDC voltage [10, 11]. Although a fault in the AC power grid on the inverter side does not cause commutation failure, owing to the limited output power on the AC side, the unbalanced power that cannot be delivered causes overvoltage of the HVDC system, and the entire HVDC system may be stopped in severe cases [12]. In a previous study [13], the response characteristics were analyzed when a fault occurred at the receiving-end AC system, but only basic strategies were used, and no improvements have been made. In [14], the structures and operation principle of LCC-VSC technology were introduced, and the dynamic response was compared between LCC-VSC technology and LCC technology on the same failure conditions. LCC-VSC technology can better stabilize the frequency and voltage of the AC system. In [15], a new control method for LCC-HVDCs was introduced, which can regulate both the direct-current (DC) voltage and the current of an LCC-HVDC system to increase the short-term operating margin of DC power transfer and improve the transient responses to DC power references. It can be used for reference for hybrid HVDC transmission systems. For multi-terminal VSC-HVDC, if the system adopts voltage-power droop control, the active power input from a non-fault rectifier station decreases to a certain extent with the increase of the DC voltage, whereas that one from a non-fault inverter station decreases with the increase of the DC system voltage after removal. This condition is conducive to the stability of the system [16] but is inapplicable for an LCC-VSC. At present, the voltage-margin control strategy is adopted in the rectifier, and the output of the overvoltage regulator is used to adjust the trigger angle of the rectifier to limit the overvoltage of the HVDC [17]. Additionally, energy-dissipation devices can be installed on the HVDC side to suppress the unbalanced power and control the high HVDC voltage [18]. However, this increases the cost of the grid and the loss of the power system.

In this study, the fault characteristics of the AC power grid on the inverter side of a hybrid HVDC transmission system are analyzed. Firstly, a hybrid HVDC transmission model is built in PSCAD on the basis of the Gezhou Dam to the Shanghai Transformation Project. Secondly,

constant-current and voltage-margin control strategies are simulated and analyzed. The simulation results show that when a three-phase metal grounding fault occurs in the AC power grid on the inverter side, overvoltage and DC interruption occur in the HVDC system. Thirdly, a DC power-balance method is proposed, and on the basis of this method, a control strategy for the overvoltage fixed trigger angle is proposed. The trigger angle on the rectifier side is set to a certain value when the HVDC voltage increases, and the unbalanced power of the VSC is reduced to the minimum extent. The proposed strategy avoids overvoltage and DC interruption of the LCC-VSC system when a fault occurs in the AC power grid on the inverter side. Finally, simulations based on Gezhouba Dam are performed to validate the effectiveness of the proposed strategy.

2 Analysis of fault characteristics of AC power grid on inverter side of hybrid HVDC transmission system

2.1 Hybrid HVDC transmission technology

A hybrid HVDC transmission system mainly includes the pole-to-pole mode (one pole using VSC and another pole using LCC) and the end-to-end mode (using an LCC at one end and a VSC at the other). The reactive power control capability of a pole-to-pole hybrid HVDC transmission system can reduce the installation of AC filters at both ends of the converter station. Additionally, the flexible HVDC transmission system can provide dynamic reactive support for the AC system at both ends, stabilize the AC bus voltage, and reduce the probability of LCC-HVDC commutation failure. This topology can be used in weak AC systems. The hybrid HVDC transmission system of this structure can achieve black start and passive operation and maximize the advantages of the two types of HVDC transmission systems. At present, it is applied in the Lu Xi Back-to-Back Project of China Southern Power Grid Co., Ltd.

The end-to-end hybrid HVDC transmission system can be divided into two modes: from the LCC to the VSC and vice versa. When a VSC is used in the inverter, the hybrid HVDC transmission system can completely avoid inverter-side commutation failure. Additionally, the AC bus voltage can be controlled by using a VSC in the rectifier. The end-to-end hybrid HVDC transmission system has advantages in the fields of new energy, such as wind power and photovoltaic grid connection. However, the AC power grid on the inverter side should be strong, and the commutation failure on the inverter side is more serious than that of the LCC-HVDC [19].

The construction of the Wu Dong De Ultra-high Voltage (UHV) Hybrid HVDC Project and the planned Gezhouba

Dam of the Shanghai Transformation Project will be performed with an LCC as the rectifier and a VSC as the inverter. In view of this scenario, the present study focuses on the transmission method with an LCC at the sending end and a VSC at the receiving end.

In a hybrid HVDC transmission system, the LCC and VSC can control the DC voltage or DC. Figure 1 shows the *U-I* external characteristics of basic control strategies, such as VSC control the DC voltage, LCC control the DC current, VSC control the DC current, and LCC control the DC voltage.

2.2 Fault characteristics of AC power grid on inverter side of hybrid HVDC transmission system

The fault in the AC power system on the inverter side of a conventional HVDC may easily cause commutation failure, which reduces the DC voltage and increases the DC current. This not only causes a current impact in the current valve but also affects the stability of the AC power grid. For a hybrid HVDC transmission system with the inverter as a VSC, the inverter side adopts the VSC converter station, and faults in the AC power system on the inverter side do not cause commutation failure. However, owing to the limited transmission power, the unbalanced power of the inverter quickly charges the VSC inverter, which causes a rapid increase in the DC voltage on the inverter side and a reduction in the DC current. At this time, to perform the constant-current control strategy, the trigger angle is reduced, and the DC voltage of the system increases greatly, leading to the increase of the voltage shock to the valve [20].

Under normal conditions, the input power to the hybrid HVDC, P_{in}, is equal to the output power of the AC system, P_{out}; Which means the unbalanced power P_b is equal to 0 [21].

$$P_{in} - P_{out} = P_b \tag{1}$$

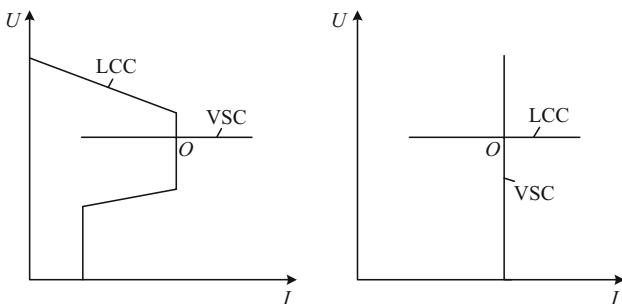When a phase contains n submodules, the DC voltage is:

$$U_{dc} = n\,u_c \tag{2}$$

where u_c is the voltage of the submodule.

According to the working principle of the submodule, the bridge arm current of phase k can be expressed as:

$$i_{pk} = C_0 \frac{\mathrm{d}u_c}{\mathrm{d}t} = C_0 \frac{\mathrm{d}U_{dc}}{n\mathrm{d}t} \tag{3}$$

where C_0 is the capacitor of submodule. The DC current is determined using the Kirchhoff current law.

$$I_{dc} = i_{pa} + i_{pb} + i_{pc} \tag{4}$$

$$I_{dc} = 3C_0 \frac{\mathrm{d}U_{dc}}{n\mathrm{d}t} \tag{5}$$

The power outputs to the VSC converter station P_{in} from the hybrid HVDC transmission system are:

$$P_{in} = I_{dc}U_{dc} = 3C_0 U_{dc} \frac{\mathrm{d}U_{dc}}{n\mathrm{d}t} \tag{6}$$

According to the instantaneous power theory, the power output to the AC system from the VSC converter P_{out} is:

$$P_{out} = 1.5U_{sd}I_{vd} \tag{7}$$

where U_{sd} is the *d*-axis component of the grid-side voltage; I_{vd} is the *d*-axis component of the current.

When a fault occurs in the inverter-side AC grid, the AC voltage decreases, and the AC current increases. U_{sd} decreases and I_{vd} increases, according to the *dq* transformation. However, because the VSC adopts the current-limiting control strategy, I_{vd} cannot increase infinitely. Therefore, the exchange active power of the VSC converter station and the AC system obtained using (7) decreases. The input power of the hybrid HVDC system to the VSC converter station is greater than that of the VSC converter station to the AC system. The DC voltage increases owing to the charging of the capacitor.

2.3 Simulation model

The hybrid HVDC transmission system shown in Fig. 2 is modeled in PSCAD using the EMTP approach. It is based on the Ge-Shang HVDC Project of China, with neutral grounding at each terminal. The rectifier side using
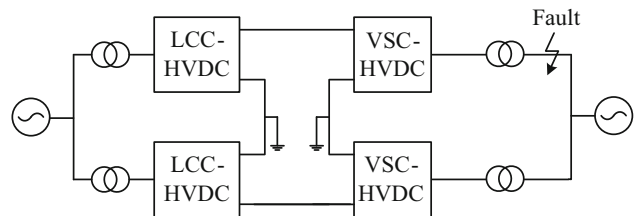

Fig. 1 *U-I* external characteristics of basic control strategies

Fig. 2 PSCAD simulation model of hybrid HVDC transmission system

the LCC is composed of a 12-pulse converter adopting a constant-current control strategy. The inverter is modeled as a ± 500 kV bipolar modular multilevel converter adopting constant-voltage control. The line adopts the frequency-dependent (phase) model. A three-phase metal grounding fault is applied in the AC power grid on the VSC side, and the AC power grid adjacent to the converter terminal is modeled by its equivalent short-circuit impedance. The windings of the converter transformer have a star configuration with a neutral ground in the AC power grid on the VSC side and a delta configuration on the converter side. The values of the system parameters are presented in Table 1.

3 Applicability analysis of voltage-margin control strategy

3.1 LCC constant-current control strategy

An HVDC transmission system usually employs the constant-current control strategy on the LCC side, and on the VSC side, the control strategy of constant voltage and reactive power is adopted. The control instruction of the LCC only has a variable trigger angle alpha when the receiving power is limited by the fault in the receiving-end AC grid. The U-I external characteristics of the LCC constant-current control strategy when a fault occurs in the receiving-end AC grid are shown in Fig. 3.

As shown in Fig. 3, during normal operation, the LCC controls the current and the VSC controls the voltage, and the normal working point is O_1. When a fault occurs in the receiving-end AC grid, the DC voltage at the receiving end increases. If the LCC continues to maintain the control strategy of the fixed current, the LCC side must reduce the trigger angle, which leads to a further increase in the DC voltage, and the working point becomes O_2. The VSC-side AC system is assumed to have a three-phase metal grounding fault at 1.5 s, and the duration of the fault is 100 ms. The simulation waveform for the case where only the constant-current control strategy is used is shown in Figs. 4, 5, 6, 7 and 8.

Figure 4 shows that the active power of the VSC output to the AC system decreases sharply after a three-phase metallic grounding fault in the AC power grid on the VSC side. The input power on the LCC side decreases slowly, and the region between the VSC input power and the output power has unbalanced energy (55.254 MJ).

Figure 5 shows that if there is no arrester on the DC side, the DC voltage on the VSC side increases rapidly after a three-phase metallic grounding fault in the VSC-side AC system, and the DC voltage of the LCC side increases rapidly through the constant-current regulation.

Table 1 Simulation model parameters

| Parameter term	Design value
Total number of bridge arm submodules	238
Rated number of bridge arm submodule	218
Redundant number of bridge arm submodules	20
Submodule-rated working voltage (V)	2293
Rated capacity of commutation valve (MW)	1500
Submodule capacitance value (mF)	15
Bridge arm reactance value (mH)	100
VSC converter transformer ratio	525/260
VSC valve side voltage (kV)	260
VSC valve side current (kA)	6.66
Fixed DC voltage K_p/K_i	8.3/0.008
Fixed reactive power K_p/K_i	1.1/0.214
Arrester DC reference voltage (kV)	5.3
Arrester residual voltage (kV)	8.01
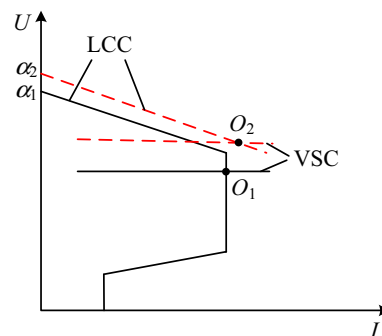
Fig. 3 U-I external characteristics of LCC constant-current control strategy

The DC voltage on the LCC side becomes lower than the AC power grid on the VSC side because the LCC side has the minimum trigger-angle limit, and DC voltage on the VSC side continues to increase owing to the current flow in the circuit.

As shown in Fig. 6, if there is an arrester on the DC side, it acts with a rapid increase of the DC voltage.

Figure 7 shows that after a three-phase metal grounding fault occurs in the the AC power grid on the VSC side, the LCC side maintains the DC voltage and DC current by reducing the trigger angle, and the trigger angle of the LCC is rapidly reduced to the minimum trigger angle.

As shown in Fig. 8, the DC decreases slowly as the constant-current control strategy on the LCC side maintains the DC voltage and DC current on the LCC side. This also improves the DC voltage on the VSC side. Therefore, if the constant-current control strategy is adopted, the DC voltage significantly increases. The results of the simulation are consistent with those of the theoretical analysis.
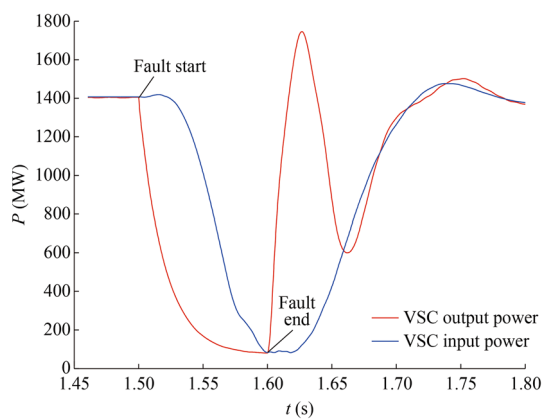
Fig. 4 Power variation of VSC-side system after a three-phase metallic grounding fault occurs in VSC-side AC system using constant-current control strategy
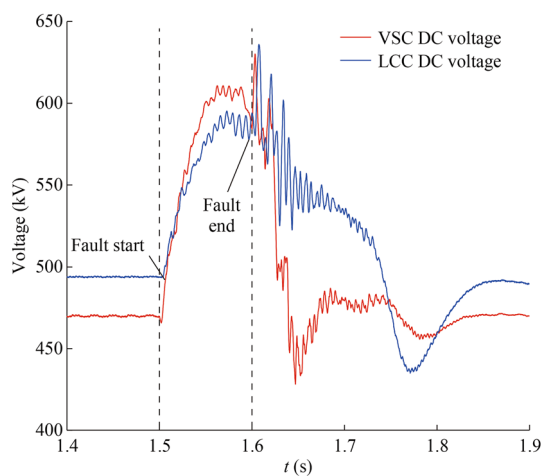

Fig. 5 DC voltage waveform after a three-phase metallic grounding fault occurs in VSC-side AC system using constant-current control strategy

Fig. 6 Current flowing through arresters using constant-current control strategy

Fig. 7 LCC-side trigger angle after a three-phase metallic grounding fault occurs in the AC power grid on the VSC side using constant-current control strategy

3.2 Voltage-margin control strategy

The voltage-margin control strategy may be used to reduce the overvoltage of the HVDC system when a fault occurs in the AC power grid on the VSC side. The voltage-margin control strategy is shown in Fig. 9.

The voltage U_{dc} between the DC line and the pole is measured in real time on the LCC side, and a voltage difference between the overvoltage threshold and low-voltage threshold is formed. The voltage deviation adjustment value is determined by the proportional–integral (PI) regulator, and the current reference value is superimposed to make the current of the entire flow station reach its target value. When the voltage difference is large, the corresponding limit link should be added to the PI controller to prevent the integral saturation. The limit link is also added to the output of the reference signal of the current in the allowable range of the capacity of the converter. When the
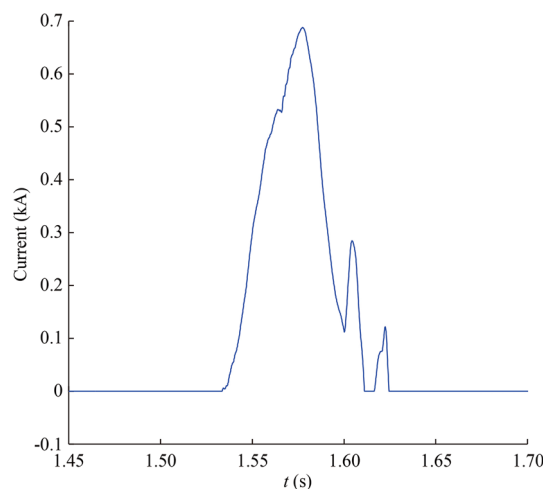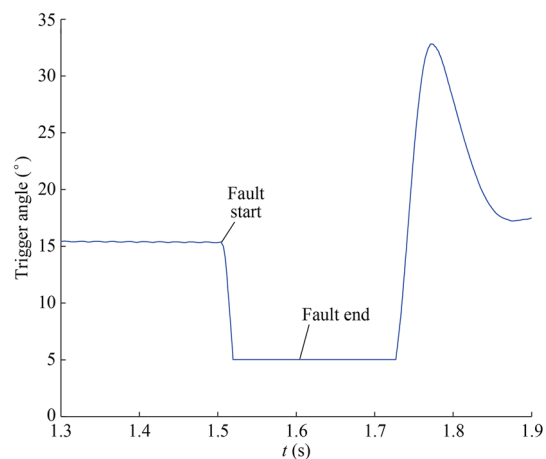
DC voltage exceeds the overvoltage threshold, the overvoltage and low-voltage modules are adjusted to the output lower limit. The voltage-margin control strategy quickly reduces the DC after the detection of the LCC DC voltage, thus maintaining the stability of the DC voltage of the system. The U-I external characteristics of the voltage-margin control strategy when a fault occurs in the receiving-end AC grid is shown in Fig. 10.

As shown in Fig. 10, during normal operation, the LCC controls the current and the VSC controls the voltage, and the normal working point is O_1. When a fault occurs in the receiving-end AC grid, the DC voltage at the receiving end increases. Additionally, on the LCC side, the reference DC and DC voltage decrease, and the working point becomes O_2.

The VSC-side AC system is assumed to have a three-phase metal grounding fault at 1.5 s, and the failure
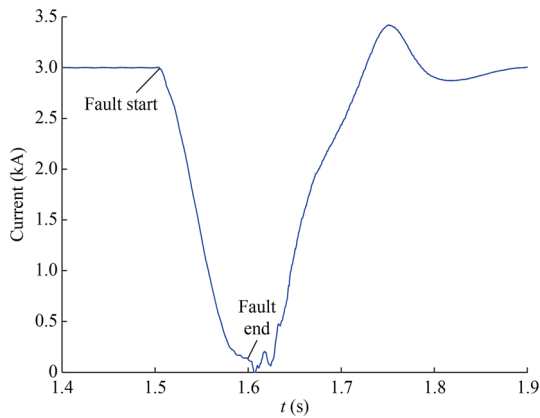
Fig. 8 DC waveform after a three-phase metallic grounding fault occurs in VSC-side AC system using constant-current control strategy
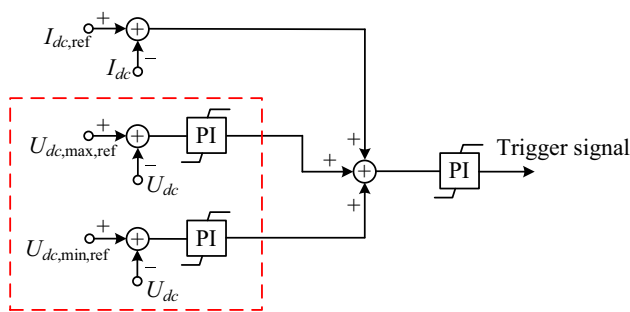

Fig. 9 Voltage-margin control strategy

Fig. 10 U-I external characteristics of voltage-margin control strategy

Fig. 11 Power variation of inverter after a three-phase metallic grounding fault occurs in the AC power grid on the VSC side using voltage-margin control strategy

Fig. 12 DC voltage waveform after a three-phase metallic grounding fault occurs in VSC-side AC system using voltage-margin control strategy

duration is 100 ms. The LCC adopts the voltage-margin control strategy. The simulation waveform is shown in Figs. 11, 12, 13, 14 and 15. Figure 11 shows that the active power of the VSC output to the AC system decreases sharply after the three-phase metallic grounding fault in the AC power grid on the VSC side. The power transported to the VSC is lower than the power during the constant-current control because the LCC side adopts the voltage-margin control strategy. The region between the VSC input power and the output power in the diagram has unbalanced energy (49.845 MJ).

Figure 12 indicates that the VSC side DC voltage increases rapidly after a three-phase metal grounding fault occurs in the VSC-side AC system. Given that the LCC side control strategy has a response delay, the control strategy begins when the LCC side DC voltage increases to 540 kV. The VSC-side DC voltage continues to increase owing to the current flow in the circuit. When the DC voltage of the LCC side is significantly smaller than that one of the VSC side, the DC is interrupted, resulting in the overvoltage on the DC system.

As shown in Fig. 13, if there is an arrester on the DC side, it acts with the rapid increase of the DC voltage.

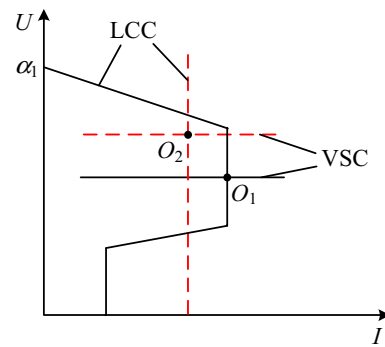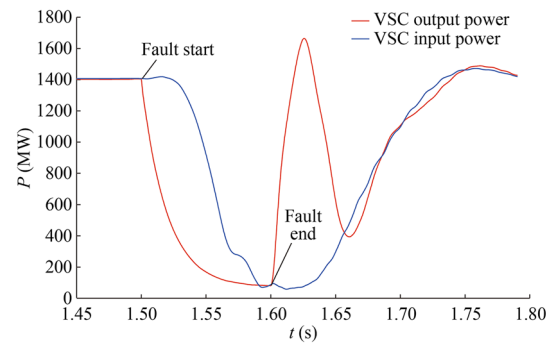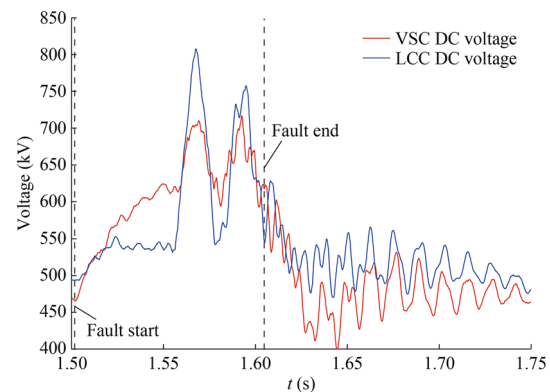Figure 14 shows that after a three-phase metal grounding fault occurs in the VSC-side AC system, the LCC side maintains the DC current by reducing the trigger angle before the voltage margin is controlled. The trigger angle of the LCC is rapidly reduced, and the DC voltage increases. After voltage-margin control is applied, the LCC trigger angle is stabilized at approximately 25° in order to normalize the voltage at a high value.
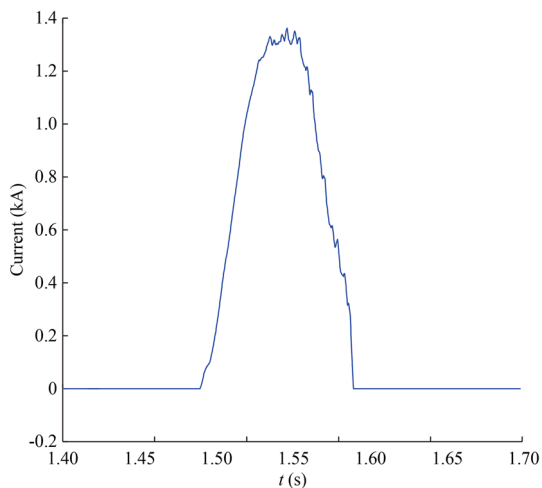
Fig. 13 Current flowing through arresters using voltage-margin control strategy
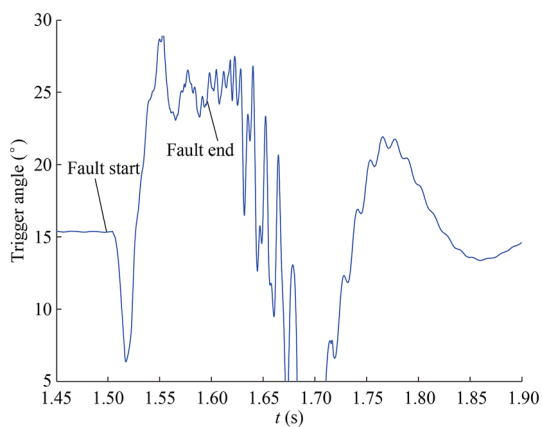

Fig. 14 LCC-side trigger angle after a three-phase metallic grounding fault occurs in VSC-side AC system using voltage-margin control strategy
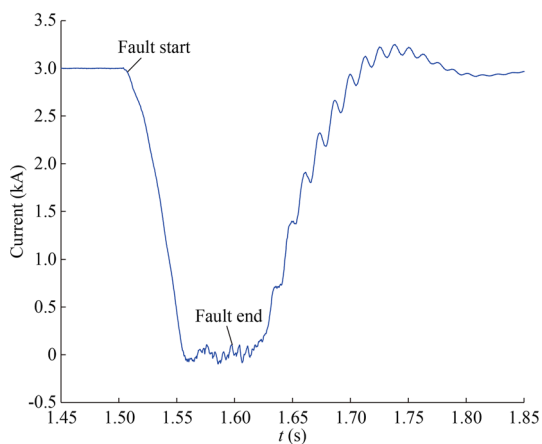

Fig. 15 DC waveform after a three-phase metallic grounding fault occurs in the AC power grid on the VSC side using voltage-margin control strategy

As shown in Fig. 15, after the voltage-margin control strategy is applied in the LCC, the voltage on the LCC side remains unchanged, but the voltage on the VSC side increases consistently and exceeds the voltage on the LCC side after a few milliseconds. With the increase of the difference between the VSC side and LCC side voltages, the DC is interrupted 50 ms after the fault, and an overvoltage of more than 1.6 p.u. is generated, which may damage the DC equipment if no measures are taken.

The comparison of the simulation results indicates that the LCC station reduces the trigger angle after the DC voltage increases when the current-control strategy is used; which causes a further increase in the DC voltage. The voltage-margin control strategy does not reduce the DC voltage significantly, owing to the response delay of the overvoltage control strategy. The DC voltage on the VSC side is significantly higher than that one on the LCC side, which causes DC interruption and overvoltage in the HVDC system.

4 Overvoltage fixed trigger angle control strategy

4.1 Structure of overvoltage fixed trigger angle control strategy

The fixed trigger angle control strategy involves a set of parallel lines with a slope of $-R_{cr}$ and the DC voltage on the rectifier side.

$$V_{dr} = V_{d0r}\cos\alpha - I_d R_{cr} \tag{8}$$

where V_{d0r} is the effective value of the rectifier side converter transformer valve no-load line voltage; α is the trigger angle; I_d is the DC; and R_{cr} is the rectifier-side equivalent commutation reactance. The formula indicates that when α increases, the DC voltage on the rectifier side decreases, hence, the DC power of the transmission can be reduced. Given that the slope of the V-I characteristic is generally small, the DC current and DC power can be significantly changed by adjusting the trigger angle.

The active power of the AC system delivered to the LCC station is given as:

$$P = EI\cos\varphi \tag{9}$$

where E is the effective value of the AC side voltage; I is the effective value of the fundamental current of the AC side; $\varphi = \alpha + \mu/2$ is the power factor angle; and μ is the overlap angle of the commutation. Ignoring the loss, the active power of the AC system delivered to the LCC station is equal to the active power output from the converter station to the receiving-end grid of the VSC. The power-balance equation is:

$$P = EI \cos \varphi = EI \cos(\alpha + \mu/2) = P_{out} = 1.5 U_{sd} I_{vd} \quad (10)$$

To control the trigger angle quickly, the trigger angle on the LCC side must be adjusted in that case the most serious fault is calculated in advance via the power-balance equation and is used as the input of the overvoltage fixed trigger angle. Lightning overvoltage generally disappears in tens of microseconds. After the LCC station detects the DC voltage exceeding the set value, the control strategy is changed from the fixed-current control to the overvoltage fixed trigger angle control strategy after the overvoltage is kept at 1 ms to avoid a false start caused by lightning overvoltage. On the LCC side, the DC is measured in real time. If the DC is interrupted, the control strategy is changed to a constant-current control strategy, and the DC is kept at the allowable level of the system. If the DC is not interrupted, the VSC side calculates the output active power according to the instantaneous power theory and transfers it to the LCC side. The trigger angle on the LCC side must be adjusted continuously according to the power balance of method while considering the communication delay. For the 1045 km line, the trigger angle can be adjusted adaptively within 20 ms after the fixed control strategy is adopted on the LCC side, which is beneficial to the stability of the system. At present, the main type of protection of the 500 kV AC system is current differential protection. Generally, the protection can be exported within 10 ms, and the circuit breaker trips within 100 ms after a fault. If no fault occurs in the AC system on the VSC side, the control strategy switches to constant-current control immediately after the AC protection information is received, with a time delay of 20 ms. If a fault occurs in the AC system on the VSC side, the LCC side switches to the constant-current control strategy after receiving the trip information for AC protection on the VSC side. A logic diagram of the overvoltage fixed trigger angle control strategy is shown in Fig. 16.

The U-I external characteristics of the overvoltage fixed trigger angle control strategy when a fault occurs in the receiving-end AC grid are shown in Fig. 17.

As shown in Fig. 17, during normal operation, the LCC controls the current and the VSC controls the voltage. The normal working point is O_1. When a fault occurs in the receiving-end AC grid, the DC voltage at the receiving end increases. In addition the trigger angle on the LCC side increases, which reduces the DC current and DC voltage. The working point becomes O_2.

4.2 Characteristics of overvoltage fixed trigger angle control strategy

A block diagram of the entire regulating system including the trigger angle regulation and regulating object, is shown in Fig. 18.
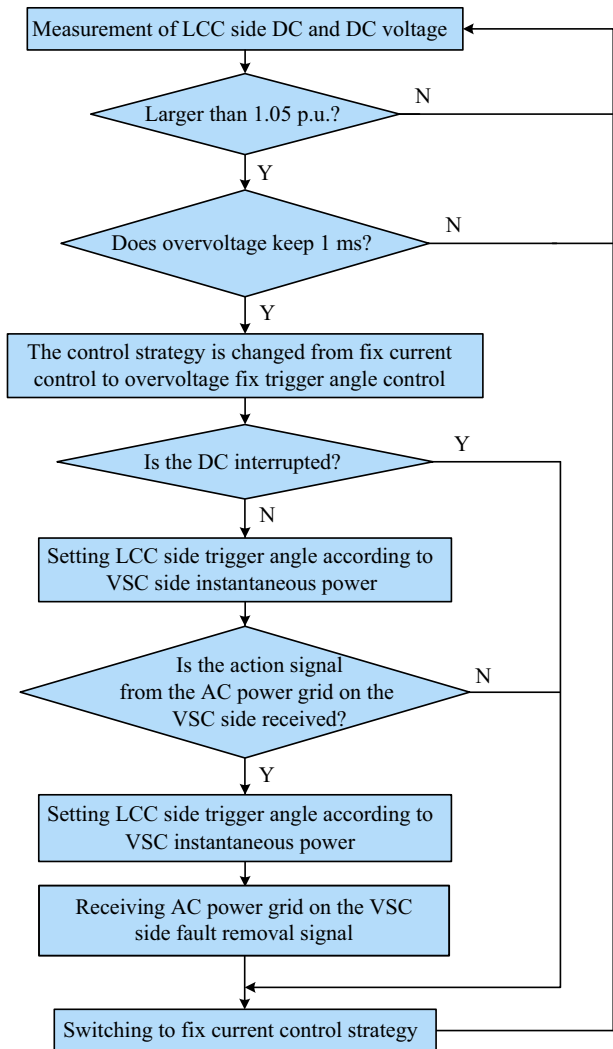

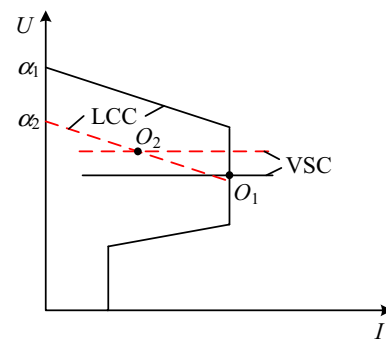Fig. 16 Logic diagram of the overvoltage fixed trigger angle control strategy

Fig. 17 U-I external characteristics of overvoltage fixed trigger angle control strategy

The overvoltage fixed trigger angle control strategy is adopted on the rectifier side, and the voltage on the inverter side is controlled. In Fig. 18, ΔV_d represents the voltage variation after a fault occurs in the VSC-side AC system,
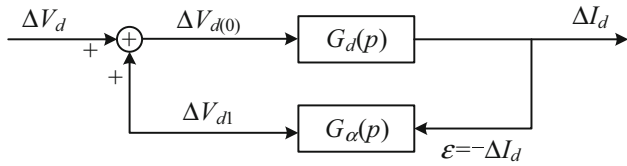
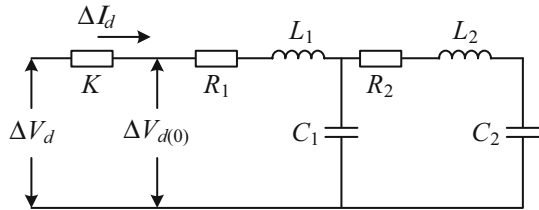**Fig. 18** Regulating system of overvoltage fixed trigger angle control strategy

Fig. 19 Equivalent circuit of HVDC system

$G_d(p)$ represents the transfer function of the HVDC system, and $G_\alpha(p)$ represents the trigger angle regulation. The transfer function of the closed-loop system under a disturbance ΔV_d is:

$$\frac{\Delta I_d}{\Delta V_d} = \frac{1}{G_\alpha(p) + \frac{1}{G_d(p)}} \tag{11}$$

$G_\alpha(p)$ is assumed to be negligible and can be simplified as K. The equivalent circuit of the HVDC system is shown in Fig. 19.

When the voltage changes ($\Delta V_{d(0)}$), the variation in the current on the HVDC line can be obtained using (12).

$$\Delta I_d = \frac{\Delta V_{d(0)}}{R_1 + pL_1 + \frac{\left(R_2 + pL_2 + \frac{1}{pC_2}\right)\frac{1}{pC_1}}{R_2 + pL_2 + \frac{1}{pC_1} + \frac{1}{pC_2}}} = \frac{\Delta V_{d(0)}}{Z(p)} \tag{12}$$

$$Z(p) = R_1 + pL_1 + \frac{\left(R_2 + pL_2 + \frac{1}{pC_2}\right)\frac{1}{pC_1}}{R_2 + pL_2 + \frac{1}{pC_1} + \frac{1}{pC_2}} \tag{13}$$

where R_1 and R_2 represent line resistance and rectifier resistance; L_1 and L_2 represent the line inductances; C_1 represents the line capacitance; and C_2 represents the inverter capacitance.

The transfer function of the HVDC system can be obtained using (14).

$$G_d(p) = \frac{\Delta I_d}{\Delta V_{d(0)}} \tag{14}$$

By combining (14) with (11), the transfer function of the closed-loop system can be simplified as:

$$\frac{\Delta I_d}{\Delta V_d} = \frac{1}{K + Z(p)} \tag{15}$$

The system characteristic equations are as follows:

$$K + Z(p) = 0 \tag{16}$$

$$a_4 p^4 + a_3 p^3 + a_2 p^2 + a_1 p + a_0 = 0 \tag{17}$$

$$a_4 = L_1 L_2 C_1 > 0 \tag{18}$$

$$a_3 = R_1 C_1 + K C_1 + R_2 L_1 C_1 \tag{19}$$

$$a_2 = R_1 R_2 C_1 + K R_2 C_1 + L_1 + L_2 + L_1 \frac{C_1}{C_2} \tag{20}$$

$$a_1 = R_1 + R_2 + K + \frac{R_1 C_1}{C_2} + \frac{K C_1}{C_2} \tag{21}$$

$$a_0 = \frac{1}{C_2} \tag{22}$$

According to the Russell Hurwitz criterion, the stability condition of the system is as follows:

$$a_3 = R_1 C_1 + K C_1 + R_2 L_1 C_1 > 0 \tag{23}$$

$$b_1 = \frac{a_2 a_3 - a_1 a_4}{a_3} > 0 \tag{24}$$

$$c_1 = \frac{b_1 a_1 - a_0 a_3}{b_1} > 0 \tag{25}$$

$$d_1 = \frac{c_1 + c_2}{c_1} a_0 > 0 \tag{26}$$

Given that $R_1 > 0$, $R_2 > 0$, and $C_1 < C_2$, all of the three conditions can be satisfied. In this case, the system is stable. According to the system parameters, the root locus of the closed-loop system is shown in Fig. 20. As $(-1 + j0)$ is not in the closed-loop circle, the system is stable.

4.3 Simulation verification

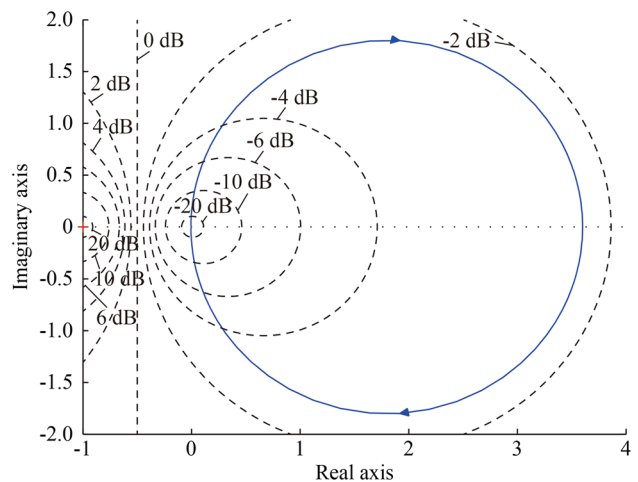A three-phase metal grounding fault is assumed to occur in the VSC-side AC system at 1.5 s, and the fault duration

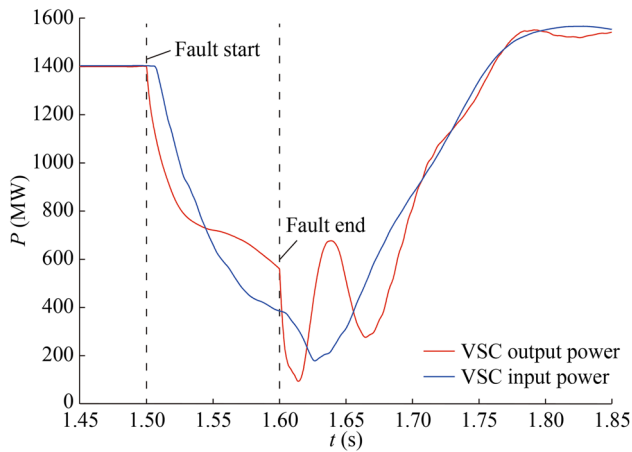**Fig. 20** Root locus of closed-loop system

Fig. 21 Power variation of VSC-side system after a three-phase metallic grounding fault occurs in VSC-side AC system using overvoltage fixed trigger angle control strategy
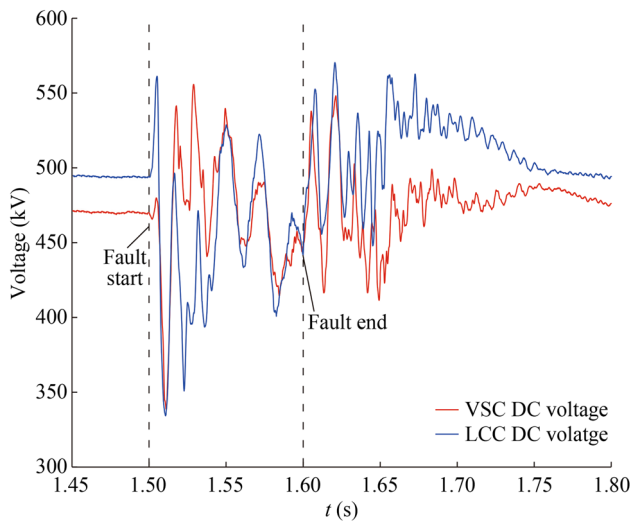

Fig. 22 DC voltage waveform after a three-phase metallic grounding fault occurs in VSC-side AC system using overvoltage fixed trigger angle control strategy

is 100 ms. The application of the overvoltage fixed trigger angle control strategy begins 1 ms after the fault occurs. The maximum trigger angle calculated via the power-balance method is 45°. Considering that the communication delay of the 1045 km line is 20 ms in a practical project, the LCC system at the sending end can adjust the trigger angle adaptively according to (10) in 20 ms after a fault occurs. The LCC side receives the fault clearing signal from the opposite system in 30 ms after the fault is cleared, and the LCC-side control strategy changes to the constant-current control. The simulation waveform for the case where the overvoltage fixed trigger angle control strategy is used is shown in Figs. 21, 22, 23, 24, 25 and 26.

Figure 21 indicates that the active power of the VSC output to the AC system decreases sharply after the three-
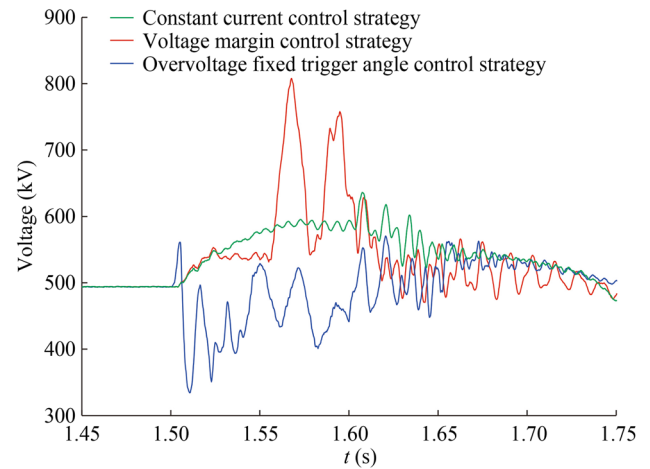

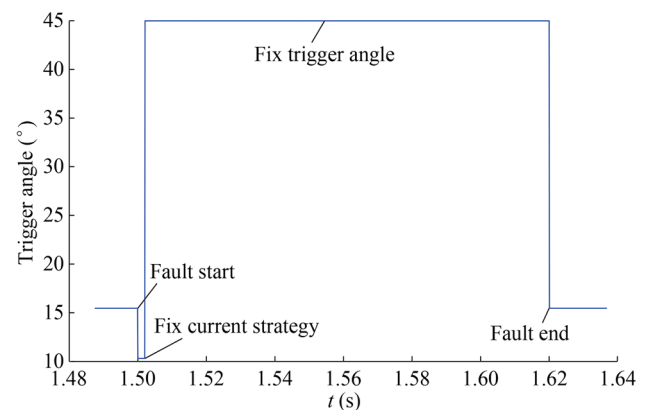**Fig. 23** DC voltage waveforms using different strategies

Fig. 24 LCC-side trigger angle after a three-phase metallic grounding fault occurs in VSC-side AC system using overvoltage fixed trigger angle control strategy
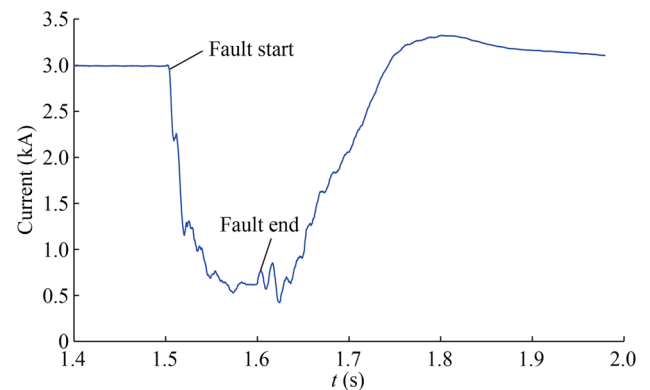

Fig. 25 DC waveform after a three-phase metallic grounding fault occurs in VSC-side AC system using overvoltage fixed trigger angle control strategy

phase metallic grounding fault in the VSC-side AC system. As a result of the LCC-side overvoltage fixed trigger angle control strategy, the LCC continuously reduces the input
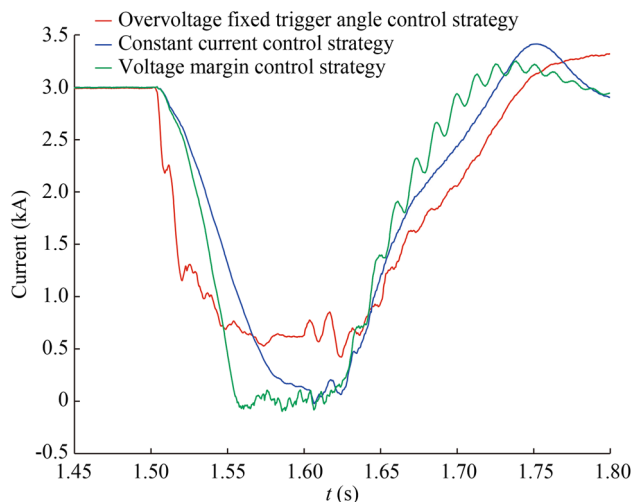
Fig. 26 DC waveform using different strategies

power and maintains the power balance between the input and output. The region between the VSC input power and the output power in the diagram has unbalanced energy, i.e., − 0.0854 MJ, which is significantly less than the unbalanced energy of 55.254 MJ using the constant-current control strategy and the unbalanced energy of 49.845 MJ using the voltage-margin control strategy.

Figure 22 shows that the VSC-side DC voltage increases rapidly after a three-phase metal grounding fault occurs in the VSC-side AC system. The DC voltage on the LCC side and the DC voltage on the VSC side decrease and are kept within the range of the system because the overvoltage fixed trigger angle triggering strategy. Under this strategy is adopted on the LCC side, the arrester does not act.

Figure 23 indicates that after a three-phase metal grounding fault occurs in the VSC-side AC system, the maximum overvoltage is 1.6 p.u. when the voltage-margin control strategy is adopted, which damages the power device. When the constant-current control strategy is adopted, the overvoltage approaches 1.2 p.u. and lasts for a long time, which reduces the safety of the power device. When the overvoltage fixed trigger angle control strategy is adopted, the overvoltage remarkably decreases. The maximum overvoltage is 1.14 p.u. and does not damage the power device.

Figure 24 shows that when a three-phase metal grounding fault occurs in the VSC-side AC system, the LCC side maintains the DC by reducing the trigger angle before the overvoltage fixed trigger angle control is applied. After the overvoltage fixed trigger angle control is applied, the LCC trigger angle stabilizes at approximately 45°.

Figure 25 shows that when a three-phase metal grounding fault occurs in the VSC-side AC system, the DC decreases rapidly and reduces the power input to the VSC

because of the overvoltage fixed trigger angle control strategy on the LCC side. Simultaneously, the strategy detects the DC interruption and can thus avoid it.

Figure 26 indicates that after a three-phase metal grounding fault occurs in the VSC-side AC system, the current decreases to zero quickly when the voltage-margin control strategy is adopted, which causes DC interruption. When the constant-current control strategy is used, the current decreases slowly and approaches zero during recovery. When the overvoltage fixed trigger angle control strategy is adopted, the current decreases quickly to reduce the overvoltage, but the current can be maintained at a certain value to avoid current interruption.

The simulation results show that after the fault occurs in the VSC-side AC system, the unbalanced power between the input and output of the VSC is relatively small because of the overvoltage fixed trigger angle control strategy of the LCC converter station. Thus, the increase in the DC voltage is effectively avoided.

5 Conclusion

A control strategy involving the overvoltage fixed trigger angle is proposed. The strategy is based on the power-balance method and reduces the overvoltage of the HVDC system after a fault in the inverter side AC system.

Firstly, the fault characteristics of the AC grid in a hybrid HVDC receiving-end transmission system are analyzed. The DC voltage increase because of the existence of unbalanced power. Secondly, a simulation model of end-to-end hybrid DC transmission is constructed on the basis of the Gezhou Dam to the Shanghai Transformation Project of China, and the applicability of the voltage-margin control strategy is analyzed. The results indicate that the voltage-margin control strategy introduces the risk of DC interruption and leads to high overvoltage. Thirdly, a DC power-balance method is proposed. According to this method, a control strategy for the overvoltage fixed trigger angle is proposed. Finally, simulations based on Gezhou Dam are performed to validate the effectiveness of the proposed strategy.

The proposed strategy is a preliminary exploration of a coordination method of system control and protection. It is a valuable reference for the research on control and protection strategies for hybrid multi-terminal HVDC systems.

References

[1] Tu JZ, Pan Y, Zhang J et al (2017) Transient reactive power characteristics of HVDC during commutation failure and impact of HVDC control parameters. J Eng 2017(13):1134–1139

[2] Marquardt R (2010) Modular multilevel converter: an universal concept for HVDC-networks and extended DC-bus-applications. In: Proceedings of the 2010 international power electronics conference-ECCE Asia, Sapporo, Japan, 21–24 July 2010, pp 502–508

[3] Lesnicar A, Marquardt R (2003) An innovative modular multilevel converter topology suitable for a wide power range, 2010. In: Proceedings of the 2003 IEEE Bologna PowerTech conference, Bologna, Italy, 23–26 June 2003, 6 pp

[4] Zhan P, Li CH, Wen JY et al (2013) Research on hybrid multi-terminal high-voltage DC technology for offshore wind farm integration. J Modern Power Syst Clean Energy 1(1):34–41

[5] Feldman R, Tomasini M, Amankwah E et al (2013) A hybrid modular multilevel voltage source converter for HVDC power transmission. IEEE Trans Ind Appl 49(4):1577–1588

[6] Jung J-J, Cui SH, Sul S-K (2017) A new topology of multilevel VSC converter for a hybrid HVDC transmission system. IEEE Trans Power Electron 32(6):4199–4209

[7] Kotb O, Sood VK (2010) A hybrid HVDC transmission system supplying a passive load. In: Proceedings of 2010 IEEE electrical power & energy conference, Halifax, Canada, 25–27 August 2010, 7 pp

[8] Li CH (2015) Research on topology and other key technologies of hybrid HVDC transmission system. Dissertation, Huazhong University of Science & Technology

[9] Perez M, Bernet S, Rodriguez J et al (2015) Circuit topologies, modeling, control schemes and applications of modular multilevel converters. IEEE Trans Power Electron 30(1):4–17

[10] Shi BN, Hong C (2017) Research on power transmission enhancement strategy of LCC-MMC hybrid HVDC system under AC symmetric fault. Power Syst Prot Control 45(20):73–79

[11] Tu QR, Xu Z, Chang Y et al (2012) Suppressing DC voltage ripples of MMC-HVDC under unbalanced grid conditions. IEEE Trans Power Deliv 27(3):1332–1338

[12] Wang PY, Zhang X-P, Coventry PF et al (2014) Control and protection strategy for MMC MTDC system under converter-side AC fault during converter blocking failure. J Modern Power Syst Clean Energy 2(3):272–281

[13] Li M, Guo Z, Cai DX et al (2018) Operating characteristic analysis of multi-terminal hybrid HVDC transmission system with different control strategies. In: Proceedings of 2018 international conference on power system technology, Guangzhou, China, 6–9 November 2018, pp 2616–2622

[14] Yu X, Yi JB, Wang N et al (2018) Analysis on dynamic response of LCC-VSC hybrid HVDC system with AC/DC faults. In: Proceedings of 2018 IEEE innovative smart grid technologies-Asia, Singapore, 1 May 2018, pp 323–327

[15] Kwon D-H, Kim Y-J, Moon S-I et al (2018) Modeling and analysis of an LCC HVDC system using DC voltage control to improve transient response and short-term power transfer capability. IEEE Trans Power Deliv 33(4):1922–1933

[16] Zhao W (2011) HVDC transmission engineering[M]. China Electric Power Press, Beijing, pp 7–9

[17] Adam GP, Ahmed KH, Finney SJ et al (2010) AC fault ride-through capability of a VSC-HVDC transmission systems. In: Proceedings of 2010 IEEE energy conversion congress and exposition, Atlanta, USA, 12–16 September 2010, pp 3739–3745

[18] Foster S, Xu L, Fox B (2008) Control of an LCC HVDC system for connecting large offshore wind farms with special consideration of grid fault. In: Proceedings of the IEEE PES general meeting-conversion and delivery of electrical energy in the 21st Century, Pittsburgh, USA, 20–24 July 2008, pp 1–8

[19] Zeng R, Xu L, Yao L et al (2015) Design and operation of a hybrid modular multilevel converter. IEEE Trans Power Electron 30(3):1137–1146

[20] Liu ZC, Shi BN, Liu B et al (2017) Control strategies of LCC-MMC hybrid HVDC transmission under AC system fault based on maximum modulation index. Autom Electric Power Syst 41(4):125–130

[21] Wang YP (2017) Research of the AC fault ride through control of VSC-MTDC. Dissertation, North China Electric Power University

Zexin ZHOU received the B.Sc. degree in Relay Protection & Automatic Remote from North China Electric Power University (NCEPU), Beijing, China, in 1991, the M.Sc. degree in Electric Power System and its Automatic from China Electric Power Research Institute (CEPRI), Beijing, China, in 1994. Now she is Director of Relay Protection Department of CEPRI, professor of engineering, doctoral supervisor. Her research interest is relay protection of electric power system.

Zhengguang CHEN received the B.S. degree in Electrical Engineering from Xi'an Jiaotong University, Shaanxi, China, in 2010, the M.S degree in Electrical Engineering from CEPRI, Beijing, China, in 2013. Currently, he is an engineer in CEPRI, China. His current research interests include power system protection and HVDC systems.

Xingguo WANG received the B.Sc., M. Sc and Ph.D. degrees from NCEPU, Beijing, China, in 2003, 2006 and 2010, respectively. He is with Power System Dynamic Simulation Laboratory, CEPRI, Beijing, China. His research interest is relay protection algorithm in power system.

Dingxiang DU received the B.Sc and M.Sc degrees in electrical engineer from NCEPU, Baoding, China, in 1999 and 2002. Currently she is a researcher in CEPRI. Her research interest is power system protection.

Guosheng YANG received the B.Sc. degree from Lanzhou University, Lanzhou, China, in 2003 and M.Sc. degree from NCEPU, Beijing, China, in 2008. Now he is a Professor-level engineer in CEPRI, Beijing, China. His research interests are power system protection and control.

Yizhen WANG received the B.E.E. degree in Electrical Engineering from Tianjin University, Tianjin, China, in 2010, the M.E.E degree in Electrical Engineering from CEPRI, Beijing, China, in 2013, and the Ph.D. degree in Electrical Engineering from Tsinghua University,

Beijing, China, in 2017, respectively. Currently, he is a Lecturer with the School of Electrical Engineering and Automation, Tianjin University, Tianjin, China. His current research interests include power system stability analysis, power system protection, and VSC-HVDC systems.

Liangliang HAO received the Ph.D. degree in fault protection for large generator, from Tsinghua University, Beijing, China, in 2012. He is an Assistant Professor in the School of Electrical Engineering, Beijing Jiaotong University Beijing. His research interests include the control and protection strategies for HVDC System.